Taylor & Francis
Taylor & Francis Group

RESEARCH PAPER

🔓 OPEN ACCESS Check for updates

Novel cross-feeding human gut microbes metabolizing tryptophan to indole-3-propionate

Janina N. Zünd[a], Denisa Mujezinovic[a], Markus Reichlin[a], Serafina Plüss[a], Marina Caflisch[a], Serina Robinson[b], Christophe Lacroix[a], and Benoit Pugin [a]

[a]Laboratory of Food Biotechnology, Department of Health Sciences and Technology, ETH Zürich, Zürich, Switzerland; [b]Department of Environmental Microbiology, Eawag, Dübendorf, Switzerland

ABSTRACT

Tryptophan-derived indoles produced by the gut microbiota, particularly indole-3-propionate (IPA), are key compounds associated with gastrointestinal balance and overall health. Reduced levels of IPA have been associated with inflammatory bowel disease, type 2 diabetes, and colorectal cancer. Since fiber-rich diets have been shown to promote IPA, we aimed to decipher fiber-specific effects and identify associated IPA-producing taxa in a range of healthy individuals. We cultured fecal microbiota from 16 adults with tryptophan and eight different dietary fibers and monitored community shifts by 16S rRNA gene amplicon sequencing and tryptophan-derived indoles using targeted liquid chromatography with diode array detection. The concentrations and types of indoles produced were donor-specific, with pectin strongly promoting IPA production in certain donors. IPA production was not associated with any known IPA producer but with the pectin-utilizing species *Lachnospira eligens*, which produced indole-3-lactate (ILA) *in vitro*, the IPA precursor. Supplementation of ILA in additional fecal microbiota cultures (*n* = 6) revealed its effective use as a substrate for IPA production. We identified a novel IPA producer, *Enterocloster aldenensis*, which produced IPA exclusively from ILA but not from tryptophan. Co-culture of *L. eligens* and *E. aldenensis* resulted in IPA production, providing new evidence for an ILA cross-feeding mechanism that may contribute to the IPA-promoting effects observed with pectin. Overall, we highlight the potential for targeted dietary interventions to promote beneficial gut taxa and metabolites.

Introduction

Metabolites produced by the human gut microbiota are important contributors to host health, serving as energy sources, cofactors, and signaling molecules.[1,2] Tryptophan-derived indoles represent one such group of microbially produced compounds with diverse signaling capabilities.[3–5] Tryptophan is degraded through a complex network of microbial pathways, including deamination to indole,[6,7] decarboxylation to tryptamine,[8,9] and transformation to indole-3-pyruvate. As part of the Stickland fermentation,[7] the latter is subsequently metabolized via an oxidative pathway to indole-3-acetate (IAA), or via a reductive pathway to indole-3-lactate (ILA), indole-3-acrylate and finally indole-3-propionate (IPA).[4,10] While indole is often associated with adverse health effects due to its conversion to indoxyl sulfate,[11] a uremic toxin contributing to chronic kidney disease pathogenesis, indole derivatives

(*e.g.*, IAA, IPA and ILA) may have numerous beneficial health effects. They have been reported to influence local and systemic processes and play a role in maintaining intestinal barrier integrity,[12,13] modulate mucin production,[14] exert antioxidant effects,[15] and orchestrate anti-inflammatory signaling through host receptors.[5,16–18] In turn, decreased indoles have been associated with inflammatory bowel diseases[19,20] as well as type 2 diabetes,[21] colon cancer[22] and multiple sclerosis,[23] among others. In particular, low levels of IPA, the end metabolite of the reductive pathway, have been identified as a prominent disease marker in several studies.[4,24–26]

Due to the beneficial effects of indole derivatives and their reduced levels in disease, there is considerable interest in further understanding microbial tryptophan pathways, particularly in promoting the reductive pathway to IPA to improve gastrointestinal

---

balance. Cohort studies have shown that tryptophan metabolism is largely influenced by dietary factors and that IPA production is strongly associated with fiber-rich diets (including fruits, vegetables, legumes, nuts, and whole grains).[27–30] In vitro and animal studies have supported the observation that certain fibers, such as non-starch polysaccharides, pectin, resistant starch, inulin, and pea, can promote IPA production.[7,31–37] Despite the observed modulation of microbial IPA production by dietary fiber, the specific fiber types, the underlying mechanisms, and the identities of the responsible bacteria remain unclear. While ILA production has been reported across diverse intestinal genera (Bifidobacterium, Lactobacillus, Bacteroides, Clostridium, Eubacterium, Faecalibacterium among others),[17,38,39] IPA production is confirmed in only a few Clostridium and Peptostreptococcus species.[12,40,41] Notably, these known IPA producers are often undetected or unlinked to the elevated IPA levels observed in in vivo studies,[29,35] suggesting that additional IPA producers remain unidentified.

In this study, we characterized IPA production from tryptophan by the healthy human gut microbiota and investigated how dietary fibers influence this process. Using anaerobic fecal microbiota cultivation in 96-deepwell plates, we screened a range of fibers to enrich the reductive pathway of tryptophan metabolism and its associated taxa. IPA levels increased in the presence of pectin, soluble starch, resistant dextrin, arabinogalactan, β-glucan, and pea fiber. Pure culture screening identified Lachnospira eligens as a novel ILA producer and Enterocloster aldenensis as a novel ILA-consuming IPA producer, suggesting an ILA cross-feeding mechanism, particularly in response to pectin supplementation. Co-culture experiments confirmed ILA cross-feeding between L. eligens and E. aldenensis. These findings highlight the potential of dietary fibers, particularly pectin, to enhance IPA production in the gut microbiota, with ILA cross-feeding as a possible underlying mechanism.

Material and methods

Growth media and anaerobic procedures

Cultivation of pure strains and human fecal microbiota was performed in 96-deepwell plates (Ritter, Schwabenmünchen, Germany) in an anaerobic chamber (10% CO_2, 5% H_2, and 85% N_2, Coy Laboratory Products Inc., Grass Lake, MI, USA) using procedures previously described in detail.[42]

To elicit strong metabolic and taxonomic responses to the tested substrates (i.e., fibers, tryptophan, ILA), we used a basal version of YCFA (bYCFA), deprived of carbohydrate sources (C-source) and containing a reduced amount of nitrogen sources (composition in Table S1)[42]. To assess indoles production, bYCFA was complemented with tryptophan or ILA to achieve final concentrations of 5 mM (for fecal cultures and co-cultures) or 1 mM (for pure strain cultures). A concentrated version of bYCFA (1.33-fold) was prepared and subsequently complemented with a range of separately prepared C-source solutions (4-fold concentrated; Table S2) to establish the final cultivation conditions within the 96-deepwell plates.

C-sources that were tested on fecal cultures included different fibers (each at final concentration of 3 gl^{-1}): arabinogalactan from larch wood (AG), inulin, beta-glucan (bGlc), pectin from citrus peel (pectin), pea fiber (pea), xylan from oat spelt (xylan), resistant dextrin (dextrin) and soluble starch from potato (starch). Alternatively, a complex C-source mixture (6C+muc; final 0.45 gl^{-1} starch, 0.45 gl^{-1} pectin, 0.45 gl^{-1} xylan, 0.24 gl^{-1} AG, 0.24 gl^{-1} guar, 1.14 gl^{-1} inulin and 0.3 gl^{-1} mucin) was used to maintain the community composition of the gut microbiota from healthy adult donors.[42] For pure strain batch cultivation, bYCFA was supplemented with a mix of three C-sources (3C) to achieve final concentrations of 1 gl^{-1} glucose, 1 gl^{-1} cellobiose and 1 gl^{-1} starch. The composition of bYCFA and the different C-source combinations are detailed in Table S1-S2.

All compounds of the bYCFA media (except L-cysteine and $NaHCO_3$) or of the C-source solutions were mixed and pH was adjusted to 7. After boiling for 10 min, the remaining compounds were added, and bYCFA media were cooled by continuous CO_2 flushing, while C-source solutions were cooled by N_2 flushing. The reduced liquids were then filled into gas-tight containers such as DURAN® Pressure flasks (DWK Life Sciences, Wertheim, Germany) or Hungate tubes (Bellco Glass, Vineland, NJ, USA) and autoclaved soon after.

Human fecal microbiota cultivation

Cultivation of fecal cultures was performed according to a detailed protocol previously reported.[42] Briefly, fresh fecal samples from 22 healthy adults (Ethics Committee of the Canton of Zurich, Project No. 2017–01290) were used, with samples from 16 donors (D1-D16) cultivated in the presence of tryptophan, and samples from 6 donors (D17-D22) cultivated in the presence of ILA. Donors reported no antibiotic use, intestinal infections, or severe diarrhea in the 3-months prior to donation. Samples were provided anonymously in plastic containers together with an Oxoid™ AnaeroGen™ bag (Thermo Fisher Scientific, Waltham, MA, USA) to create low-oxygen conditions. Samples were then transferred to the anaerobic chamber within 3 h for further processing. Cultivation conditions were established in 96-deepwell plates by adjusting the starting pH of bYCFA to 6.5 using 3 M HCl. Right after, each well was filled with 1.5 ml of bYCFA and complemented with 0.5 ml of the respective C-source solution (2 ml final volume). Finally, fecal dilutions at 10^{-4} (in anaerobic phosphate buffer) were inoculated (1% v/v, technical triplicates). Contamination controls without inoculum were placed at the plate edges and visually monitored for any undesired microbial growth. Following a 48-h incubation period within the anaerobic chamber (37°C), the optical density (OD_{600}) of the cultures (200 μl in 96-well plates) was assessed using a Tecan Infinite M200 PRO plate reader (Tecan Group Ltd., Männedorf, Switzerland). For subsequent community and metabolic analyses, we pooled technical replicates (each 0.5 ml) and centrifuged the resulting sample pools (5'500 rpm, 20 min, 4°C) to recover supernatants and cell pellets, which were stored separately at −80°C until further use.

Pure intestinal strain cultivation

The tryptophan- and ILA-metabolizing capacity of potential indoles-producing strains ($n = 17$) was tested in pure batch cultures. Intestinal strains listed in Table S3 were obtained from the German Collection of Microorganisms and Cell Culture GmbH (DSMZ, Braunschweig, Germany) and the American Type Culture Collection (ATCC, Manassas, VA, USA). Additionally, we included two of our isolates: *Enterocloster* sp. FBT_B and *E. aldenensis* FBT_C (formerly *Clostridium aldenense*). These isolates were derived from enrichment cultures of a healthy human microbiota (female, age 28) in bYCFA-3C supplemented with 20 mM tryptophan. In brief, after two incubation periods of 48 h, culture dilutions were spread on agar plates (bYCFA-3C with 20 mM tryptophan), followed by several rounds of colony picking and re-inoculation until pure cultures were obtained. The purity of the isolates was assessed by Gram staining and 16S rRNA gene sequencing using Sanger sequencing (Eurofins Scientific, Luxembourg, Luxembourg; GenBank accessions PQ060500 and PQ060501).

All strains were preserved at −80°C in 25% (v/v) anaerobic glycerol stocks and reactivated by inoculating (1% v/v, biological triplicates) bYCFA-3C medium filled into 96-deepwell plates and incubating for 24 h at 37°C within an anaerobic chamber. Active pre-cultures were inoculated (1% v/v, biological triplicates) into bYCFA-3C medium containing 1 mM of tryptophan or ILA. After 48 h incubation (37°C), we assessed growth (OD_{600}) and culture supernatants were collected by centrifugation (5'500 rpm, 20 min, 4°C) and further processed for indoles metabolite analysis.

Indoles quantification using ultra-high performance liquid chromatography

Tryptophan-derived indoles (*i.e.*, indole, IAA, ILA and IPA) were quantified using Ultra-High Performance Liquid Chromatography (UHPLC) coupled to a Diode Array Detector (DAD), with modification from a previously reported method.[43] Proteins were precipitated from the samples to improve the baseline by mixing 100 μl of culture supernatant with 100 μl acetonitrile. Following thorough mixing, the suspension was centrifuged for 5 min at 5500 rpm, 4°C. Subsequently, 130 μl of the supernatant was mixed with 130 μl MilliQ H_2O, transferred to a 0.2 μm nylon membrane filter (AcroPrep™ Filter Plates; VWR International, Radnor, PA, USA), and centrifuged at 55,000 rpm,

4°C, for 4 min. The filtrates were recovered and stored at 4°C until analysis.

Samples were analyzed using a Vanquish Flex UHPLC-DAD system (at 280 nm; Thermo Fisher Scientific). The separation was performed at 25°C using a SecurityGuard ULTRA Cartridges UHPLC F5 (Phenomenex Inc, Basel, Switzerland) connected to a Kinetex® F5 column (2.6 µm particle size; 2.1 × 100 mm; Phenomenex Inc.). Samples (1 µl injection) were eluted with a gradient of methanol with 0.015% formic acid (eluent A) and MilliQ H_2O with 0.015% formic acid (eluent B) as follows (flow rate 0.15 ml/min): 0–1 min [A 0%, B 100%]; 1–2.5 min [A 0–73%, B 100–27%]; 2.5–8 min [A 73–30%, B 27–70%]; 8–11 min [A 30–73%, B 70–27%]; 11–11.5 min [A 73–77%, B 27–23%]; 11.5–12 min [A 77–90%, B 23–10%]; 12–13 min [A 90–73%, B 10–27%]; 13–14 min [A 73–4%, B 27–96%]; 14–16 min [A 4–0%, B 96–100%]; 16–17 min [A 0–90%, B 100–10%]; 17–18.5 min [A 90%, B 10%]; 18.5–21 min [A 90–0%, B 10–100%]; and 21–30 min [A 0%, B 100%]. Concentrations of indoles were determined using external standards: Indole (I3408), DL-Indole-3-lactic acid (I5508), and 3-Indolepropionic acid (220027) were purchased from Sigma-Aldrich Chemie GmbH (Buchs, Switzerland), and Indole-3-acetic acid (A10556–06) was purchased from Thermo Fisher Scientific. Peaks for indole, IAA, ILA and IPA (Figure S1A) were integrated, and data were processed using the Chromeleon 7.2 software (Thermo Fisher Scientific). Standards showed linearity with R^2 >0.99 over the concentration range of 0.0005 to 0.2 mM (Figure S1B). The Limit of Detection (LOD), calculated as $3 \times (\sigma/S)$ (where S is the slope of the linear regression and σ is the standard deviation of the calibration curve), averaged 2.5 µM across all indoles.

Tryptamine was quantified using another UHPLC-DAD method for the quantification of neurotransmitters as previously detailed.[44] Tryptamine hydrochloride (246557, Sigma Aldrich) was used as an external standard.

DNA extraction and community analysis using 16S rRNA gene amplicon sequencing

Cell pellets were mixed with 1 ml CTAB (cetyltrimethylammonium bromide, Maxwell® RSC PureFood GMO and Authentication Kit, Promega, Madison, WI, USA), transferred to Lysing Matrix E Tubes (MP Biomedicals, Illkirch-Graffenstaden, France) and incubated for 5 min at 95°C. Subsequently, mechanical lysis of cell pellets was performed using and the FastPrep homogenizer (FastPrep-24TM; MP Biomedicals) with two cycles of 40 sec (6.0 m/sec, pause 5 sec). Samples were treated with 40 µl Proteinase K and 20 µl RNase A (Maxwell® RSC PureFood GMO and Authentication Kit), mixed by inversion for 30 sec, and incubated at 70°C for 10 min. Following incubation, samples were centrifuged at 10,600 rcf for 5 min. The DNA from fecal cultures incubated with tryptophan was further purified using the Maxwell® RSC instrument and the Maxwell® RSC PureFood GMO and Authentication Kit (Promega). The DNA from fecal cultures incubated with ILA was processed using the KingFisher Flex instrument (Thermo Fisher Scientific) and the Maxwell® HT 96 gDNA Blood Isolation Kit (Promega). Aiming for a high taxonomic resolution, the sequencing library with DNA from the tryptophan screening was prepared by amplification and barcoding of the V3-V4 hypervariable region of the 16S rRNA gene through polymerase-chain reaction (PCR) with the primers 341F (5'-CCTACGGGNBGCASCAG-3') and 806bR (5'- GGACTACNVGGGTWTCTAAT-3') by the sequencing provider (StarSeq, Mainz, Germany). A shorter region (V4 only) was amplified and barcoded from DNA originating from the ILA screening using the barcoded primers 515F (5'-GTGCCAGCMGCCGCGGTAA-3') and 806 R (5'-GGACTACHVGGGTWTCTAAT-3') (Integrated DNA Technologies, Leuven, Belgium) (Caporaso et al., 2011, 2012). The libraries were sequenced using the Illumina MiSeq platform and the corresponding amplifying primers at StarSeq or at the Genetic Diversity Centre (ETH Zurich, Switzerland).

For processing of the demultiplexed sequencing reads, we used the metabaRpipe R package (v0.9)[45] and the DADA2 R package (v1.14.1).[46] The reads from the tryptophan and ILA data sets were truncated at positions c(240,220) and c(160,140), respectively, and the maximum error rates were set to c(3,4) and c(2,2). The minimum overlap for read merging was set to 25. Taxonomy was assigned to the based on the

SILVA database (v138.1).[47,48] Sequencing reads were further analyzed using the phyloseq package (v1.40.0)[49] and the R software (v4.2.0). Reads from the tryptophan and ILA screening were rarified to 3121 and 3643 reads, respectively. For illustrating the taxonomic distribution of the complex community composition, comp_barplot() from the microViz package (v0.10.8) was used.[50] To identify taxa potentially associated with IPA production, 16S rRNA gene sequences of known IPA producers (Table S4-S5) were aligned to ASVs present in the data set using Basic Local Alignment Search Tool (BLAST).[51]

Genome analysis for the reductive pathway of tryptophan metabolism

Publicly available genomes of newly identified ILA- and IPA-producing species were accessed for the genes involved in IPA production. Specifically, the genomes of *Clostridium sporogenes* ATCC 15579 (GCF_000155085.1), a well-studied IPA-producing human isolate, and *L. eligens* DSM 3376 (GCF_000146185.1) were retrieved (May 2024) from the National Center of Biotechnology Information (NCBI) assembly database. A genome of a human *E. aldenensis* strain (GUT_GENOME001547) was accessed (May 2024) from the HumGut database.[52] The genomes were annotated using rapid prokaryotic genome annotation (Prokka).[53] Then, a homology-based search of the amino acid sequences of the *C. sporogenes* ATCC 15575 gene cluster responsible for the reductive pathway (CLOSPO_RS01525 to CLOSPO_RS01570) was performed on the genomes of *L. eligens* and *E. aldenensis* using the blastp algorithm. The location and genetic environment of the homologs were then visualized using CLC Genomic Workbench (v24.0, QIAGEN, Aarhus, Denmark).

Data analysis and visualization

Data analysis and visualization were done using the R software (v4.2.0) and the ggplot package (v3.3.6).

Prior to statistical testing, data normality was assessed using the Shapiro – Wilk test. To detect significant differences between groups, we performed either a t-test (for parametric data) or a Wilcoxon test (for non-parametric data) using the rstatix package (v0.7.0). When comparing different treatments on the same donor microbiota, paired statistics were applied. If not stated otherwise, the Holm – Bonferroni method was used to correct p-values for multiple testing.

Metabolite concentrations were correlated (Pearson correlation) with center-log ratio (clr) transformed abundances (zeros handled by adding a pseudocount) of all detected ASVs (donor-wise analysis). Data were clr-transformed using 1000 Dirichlet Monte Carlo instances. All ASV–metabolite correlations with $p < 0.05$ were reported. Due to the high number of comparisons, correction for multiple testing was not applied.

To evaluate the differential abundance of specific taxonomic groups, we performed ALDEx2 using the aldex.clr function from the mia package (v1.5.17).[54] Significantly altered taxa were identified based on the p-value of the Welch's t-test, corrected according to the Benjamini–Hochberg method.

Results

Fibers promote IPA production by fecal microbiota cultures from healthy adults

We first aimed to determine whether specific fiber types could promote the production of indoles in a wide range of individuals' gut microbiota. We cultivated 16 diverse fecal-derived human microbiota (Figure S2A-B) in the presence of tryptophan (5 mM), and supplemented the cultures with either starch, xylan, AG, bGlc, inulin, dextrin, pectin, pea (3 gl^{-1} each) or H_2O as control (Figure 1(a)). No indoles were detected in the non-inoculated medium (Figure S1C-D).

After 48 h, all fecal cultures showed tryptophan conversion with the detection of IPA, ILA, IAA, indole and tryptamine (Figure S2C-D). However, the amount and type of indoles produced varied depending on the type of fiber supplemented and the donor microbiota (Figure S2). After normalizing metabolite levels to account for biomass differences across treatments (endpoint OD$_{600}$; Figure S2E), specific IPA production was significantly promoted by starch, dextrin, AG, bGlc, pectin, and pea fiber compared to the negative control
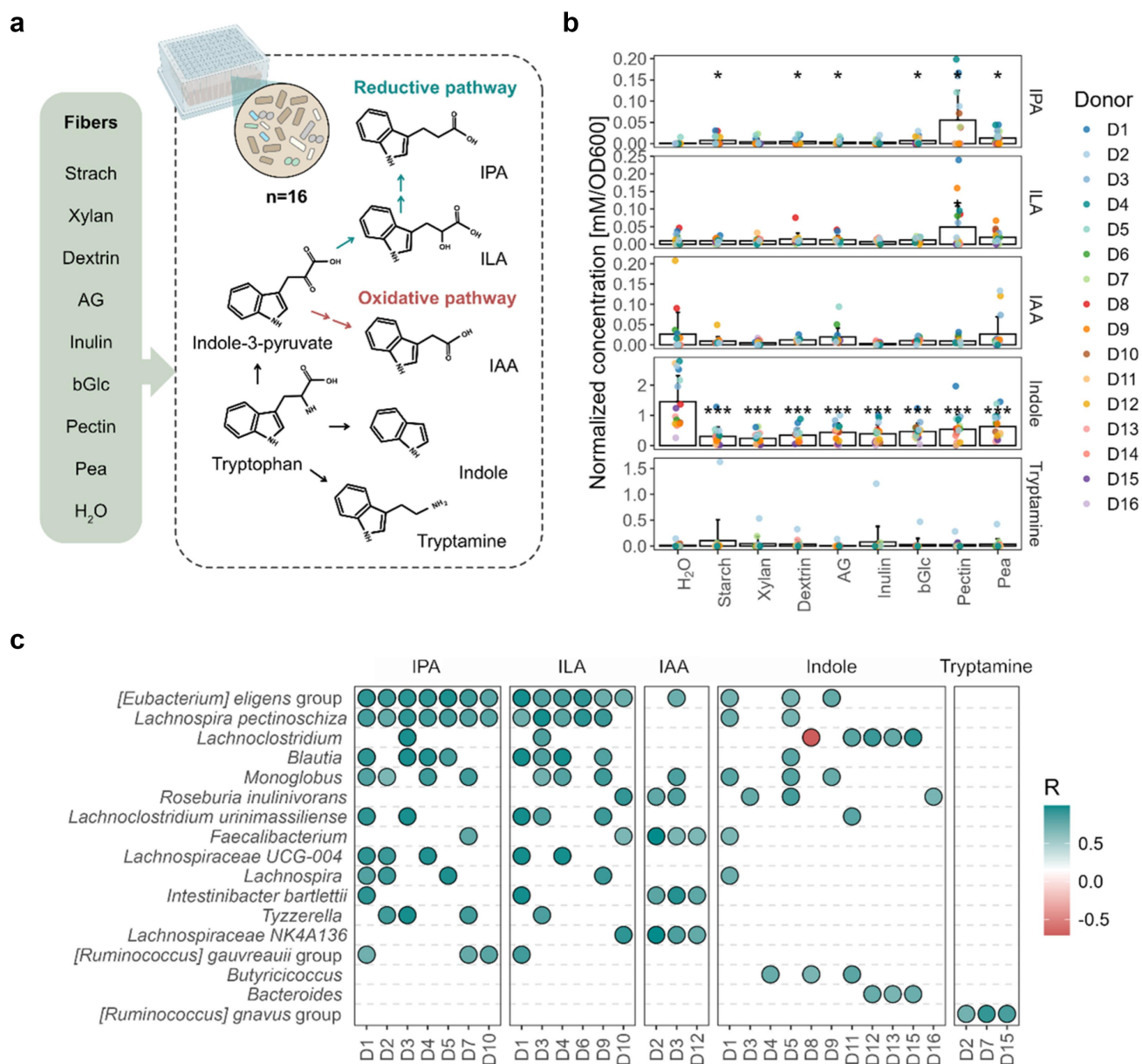
Figure 1. Effect of fiber supplementation on indoles production during fecal cultivation with healthy donor microbiota. (a) Overview of the tested fibers (3 gl^{-1}; starch, xylan, AG, bGlc, inulin, dextrin, pectin, pea or H_2O), the detected indoles and respective metabolic pathways. Red arrows highlight the oxidative, and blue arrows the reductive pathway. (b) The specific concentrations (relative to endpoint OD_{600}) of indoles detected in supernatants of fecal microbiota cultures ($n = 16$ donors) at the end of the fermentation (48 h, 37°C). Limit of detection: 2.5 µM across all metabolites. Bars represent means, and error bars represent standard deviations. Comparisons of fiber-supplemented cultures and negative controls (H_2O) were done using a paired Wilcoxon test. Statistically significant results are marked by stars, with *$p \leq 0.05$, **$p \leq 0.01$. (c) Metabolite-ASV correlations in fecal cultures fecal of healthy donor microbiota supplemented with tryptophan (5 mM). Positive ASV-metabolite correlations ($p \leq 0.05$) detected in at least three donor microbiotas were assigned to the corresponding taxonomic group at species level. Due to the large number of comparisons, no multiple testing correction was applied. Each circle represents the correlation result for one ASV in one donor microbiota, with color indicating the Pearson correlation coefficient (R).

(H_2O; $p \leq 0.05$, paired Wilcoxon test; Figure 1(b)). The highest absolute IPA production was observed with pectin (34.3 ± 42.7 µM), followed by pea fiber (10.0 ± 12.3 µM), starch (6.1 ± 8.6 µM), bGlc (6.0 ± 7.6 µM), dextrin (4.0 ± 6.4 µM), and AG (2.3 ±

3.5 µM; Figure S3). The strong response to pectin was primarily driven by IPA production in eight donor microbiotas (D1–D5, D7, D8, D10), while in the remaining donors (D6, D9, D11–D16), IPA levels were below the detection limit (LOD:

2.5 µM), highlighting the influence of baseline microbiota composition (Figure S2B).

ILA production was also significantly promoted by pectin compared to the negative control in biomass-normalized data ($p \leq 0.05$, Figure 1(b)) and was primarily driven by seven donor microbiotas (D1–D4, D6, D8, D9). When considering absolute concentrations, in addition to pectin (30.1 ± 42.5 µM), pea fiber (14.2 ± 12.5 µM), dextrin (11.8 ± 14.5 µM), AG (10.0 ± 9.5 µM), bGlc (9.2 ± 5.3 µM), and starch (7.9 ± 5.5 µM) also appeared to significantly promote ILA levels compared to fiber-depleted conditions (H_2O; 2.9 ± 4.6 µM; Figure S3), though differences may partly reflect biomass differences.

Notably, all fibers led to a general decrease in the specific production of indole compared to the fiber-depleted condition ($p \leq 0.001$; Figure 1(b)), which remained significant in absolute concentrations for starch, xylan, and dextrin ($p \leq 0.01$; Figure S3).

Finally, tryptamine was only produced at high levels by microbiota D2 and reached maximal levels under the starch condition (1.13 mM; Figure S3).

Taken together, these data highlight the donor microbiota-specific metabolism of tryptophan, which is further modulated by the presence of dietary fiber (Figure 1(b)).

Lachnospira eligens is an ILA-producing species promoted by pectin

Next, we sought to identify the taxa specifically associated with elevated IPA production using 16S rRNA amplicon sequencing. Interestingly, none of the known IPA-producing species (*i.e.*, *Clostridium* spp. and *Peptostreptococcus* spp. listed in Table S4) could be detected in our dataset using the SILVA-based annotations, nor by aligning the detected ASVs with the 16S rRNA sequences of known IPA producers using BLAST. High sequence similarity was found only for *Clostridium paraputrificens* (>97%; Table S4), but the clr-abundance of the corresponding ASVs (*i.e.*, ASV0416, ASV2820, ASV1148, ASV0571) was low (−0.10 ± 0.17) and did not significantly correlate with IPA levels ($R = -0.06$, $p = 0.186$; Figure S4).

Therefore, we further investigated whether indoles concentrations could be associated with the abundance of any of the detected ASVs, potentially revealing novel indoles producers. Pearson correlation analysis between metabolite levels and clr-abundances of each ASV revealed several taxonomic groups that were positively correlated with indoles (Figure 1(c)). This analysis showed known taxon-metabolite associations, such as tryptamine with *[Ruminococcus] gnavus* group[8] and indole-3-acetate with *Intestinibacter bartlettii* (formerly *Clostridium bartlettii*).[39] Additionally, we found positive correlations between IPA and/or ILA and ASVs assigned to the *[Eubacterium] eligens* group (reclassified as *Lachnospira eligens*), and *Lachnospira pectinoschiza* particularly in microbiotas D1–D7, D9, and D10 (Figure 1(c)), largely overlapping with the donors in which pectin strongly promoted ILA and IPA levels (Figure 1(b)). Consistently, both taxa are known for their pectin-degrading capabilities[55,56] and showed significant enrichment in pectin- and pea fibers-supplemented cultures compared to fiber-depleted conditions (Figure S5). Notably, pea fiber contains significant amounts of pectin, a major component of pea cell walls.[57]

To assess the potential for indoles production in those pectin-associated taxonomic groups, we analyzed the supernatant from pure cultures of *Lachnospira eligens* DSM 3376 and *Lachnospira pectinoschiza* DSM 116431. When grown with 1 mM tryptophan (37°C, 48 h), *L. eligens* produced ILA (0.18 ± 0.06 mM) but not IPA (Figure S6). In contrast, *L. pectinoschiza* produced neither ILA nor IPA (LOD: 2.5 µM; Figure S6). Taken together, we identified a new ILA-producing species that is promoted by pectin in fecal communities.

ILA is converted to IPA by fecal microbiota and Enterocloster aldenensis

The identification of a novel ILA producer that correlated with IPA levels led us to hypothesize that the pectin-mediated increase in IPA production could be driven by the enrichment of

Lachnospira species, some of which produce ILA. In turn, this ILA could be taken up and converted to IPA by other species. Some known IPA producers (*e.g., Clostridium sporogenes*) have previously shown the ability to take up ILA and produce IPA.[4] However, these species could not be detected in our fecal cultures screened under a wide range of conditions (16 donors and 8 fibers; Table S4).

To first assess whether ILA-to-IPA conversion is a common feature of the healthy adult gut microbiota, we tested the microbiota from six new donors. Fecal cultures were supplemented with 5 mM ILA, and either pectin (3 gl^{-1}), a complex mixture of carbon sources (6C+muc; 3 gl^{-1} total), or H_2O (negative controls) to investigate whether pectin also promotes ILA conversion to IPA (Figure 2(a)).

All fecal microbiota cultures converted ILA to IPA, with a mean stoichiometric conversion rate of $41.0 \pm 23.2\%$, yielding millimolar concentrations (Figure 2(a)), exceeding the micromolar levels observed in tryptophan-supplemented cultures (Figure 1(b)). In contrast, no IPA was detected in cultures lacking ILA, confirming that its presence is essential for IPA production (Figure 2(a)). However, IPA production from ILA was not significantly enhanced by pectin (3.03 ± 1.92 mM) compared to a complex C-source mix (2.28 ± 1.14 mM) or H_2O alone (2.15 ± 0.88 mM; Figure S7), suggesting that the taxonomic groups responsible for ILA to IPA conversion were not consistently enriched by pectin.

Given the high prevalence of ILA consumption across distinct microbiota and, again, the absence of known IPA producers in these fecal cultures (Table S5), we investigated whether we could identify novel taxa capable of converting ILA to IPA by screening a larger panel of pure intestinal strains ($n = 17$). We focused our selection on taxonomic groups that correlated with IPA production in fecal cultures supplemented with tryptophan (Figure 1(c), Table S6) or ILA (Figure S8, Table S7), and included the known IPA producer *C. sporogenes* ATCC 15579 as a positive control. After 48 h growth in the presence of 1 mM tryptophan, IPA production was undetectable for all strains except *C. sporogenes* (1.028 ± 0.165 mm; Figure 2(b)). With 1 mM ILA supplementation, IPA was produced by *C. sporogenes* (0.420 ± 0.059 mM), and by two novel IPA-producing strains of the species *Enterocloster aldenensis* (DSM 19262: 0.596 ± 0.002 mM; FBT_C: 0.578 ± 0.078 mM; Figure 2(b)). These *E. aldenensis* strains were selected based on the alignment of their 16S rRNA gene (>97%) with the sequence of ASV0066 (D19 and D21) and ASV0086 (D21 and D18), which showed correlations with IPA levels in ILA-supplemented cultures of donor microbiota (Figure S8, Table S7).

Cross-feeding between the ILA-producing *L. eligens* and the IPA-producing *E. aldenensis*

The discovery of human intestinal strains that metabolize ILA to IPA but not tryptophan to IPA (Figure 2(b)) supports the hypothesis of cross-feeding mechanisms along the reductive pathway of tryptophan metabolism. To confirm ILA cross-feeding between the identified ILA- and IPA-producing strains, we cultivated *L. eligens* DSM 3376 and *E. aldenensis* FBT_C in single and co-cultures in bYCFA containing 1 mM tryptophan and a mixture of C-sources (3C) or pectin (44 h, 37°C; Figure 2(c)). No IPA was produced in single cultures, whereas ILA accumulated with *L. eligens* (3C: 0.44 ± 0.20 mM; pectin: 0.29 ± 0.02 mM), and indole with *E. aldenensis* (3C: 0.8 ± 0.05 mM; pectin: 0.43 ± 0.38 mM). In co-cultures with 3C, IPA production reached 0.21 ± 0.18 mM (Figure 2(c)), with a large standard deviation due to one replicate lacking *L. eligens* and no IPA detected (Figure S9). On the contrary, pectin supplementation favored *L. eligens*, allowing reproducible co-cultivation with *E. aldenensis* and resulting in IPA production of 0.33 ± 0.02 mM (Figure 2(c), Figure S9).

Genes of the reductive pathway of tryptophan metabolism in *L. eligens* and *E. aldenensis*

After identifying two novel species that are highly prevalent in the human population (>75% across more than 5700 healthy human gut metagenomes; Figure S10A) and phylogenetically distinct from known ILA and IPA producers (Figure S10B), we conducted a genome analysis to identify the enzymes involved in the conversion of tryptophan to ILA (*L. eligens)* and ILA to IPA (*E. aldenensis;* Figure 3(a)). We performed a homology-based analysis using the genome of the well-studied IPA
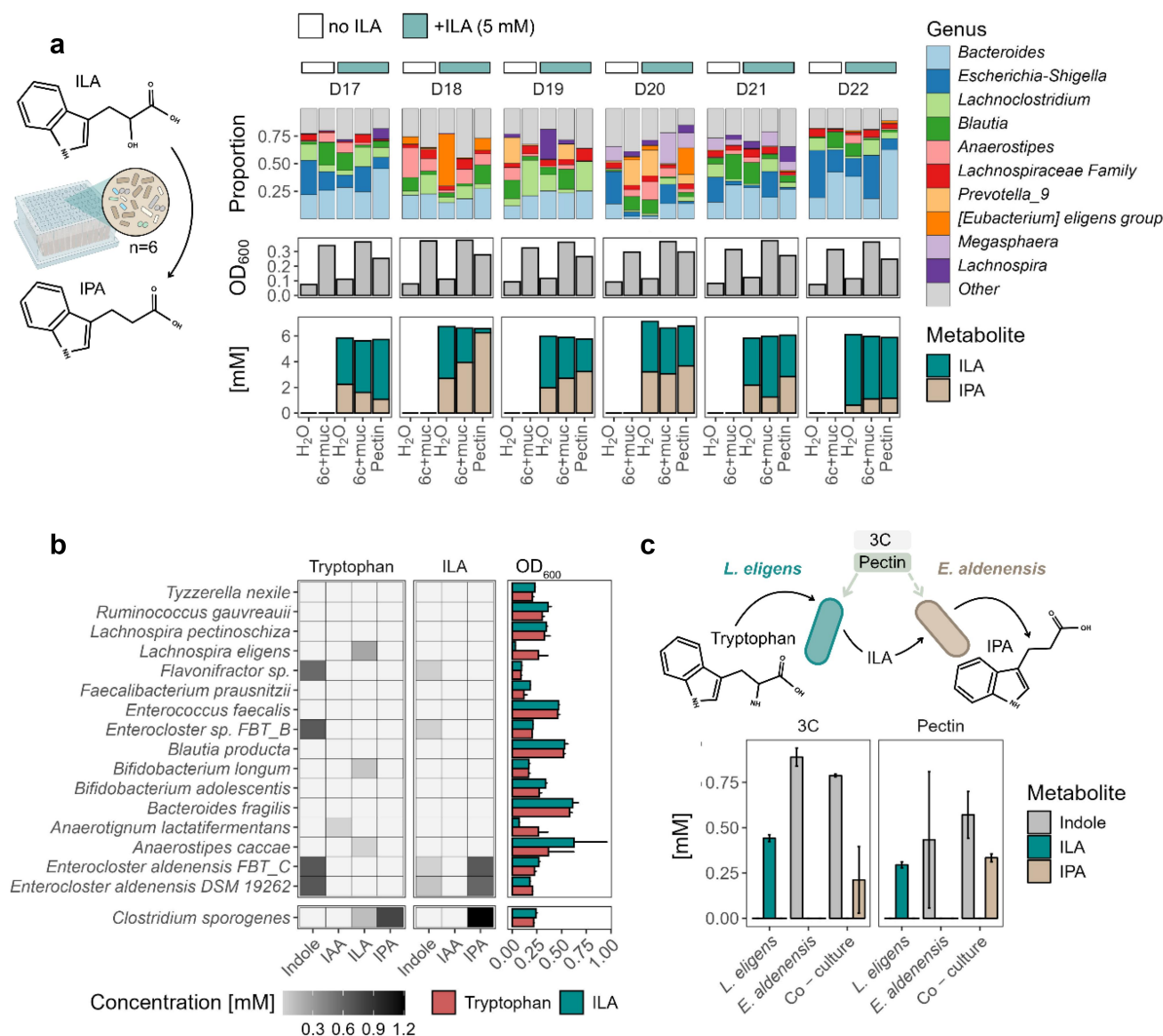
Figure 2. Conversion of ILA to IPA in fecal microbiota cultures from healthy donors and pure intestinal strains. (a) Fecal microbiota (*n* = 6 donors) were incubated (37°C, 48 h) in bYCFA supplemented with 5 mM ILA and two different C-source combinations (6C+muc, pectin) or H_2O as control. Controls without ILA were included for 6C+muc and H_2O. Fecal microbiota cultures were analyzed for community composition, growth (OD_{600} in 200 µl) and metabolite concentrations. b) Indoles production and growth (OD_{600} in 200 µl) in pure batch cultures supplemented with 1 mM tryptophan or ILA (in bYCFA-3C, 48 h, 37°C). All 17 strains were tested in biological replicates (*n* = 3). C) Indole metabolite production from tryptophan in single and co-cultures of *L. eligens* DSM 3376 and *E. aldenensis* FBT_C. The data represent biological replicates (*n* = 3).

producer *C. sporogenes* ATCC 15579 (NCBI: GCF_000155085.1). The genes responsible for the reductive pathway in *C. sporogenes* are well characterized and grouped in a conserved gene cluster, except for the amino acid transferase that performs the first step of the conversion of tryptophan to indole-3-pyruvate. (Figure 3).[4,58,59] Key enzymes and corresponding genes include the phenyllactate dehydrogenase (*fldH*; indole-3-pyruvate to ILA conversion, CLOSPO_RS01570), the phenyllactate dehydratase enzyme complex (*fldLAIBC*: ILA to indole-3-acrylate conversion, CLOSPO_RS01525 to CLOSPO_RS01545) and the acyl-CoA dehydrogenase (*acdA*; indole-3-acrylate to IPA conversion, CLOSPO_RS01550), forming an enzyme complex with electron transfer factors (*etfAB*,
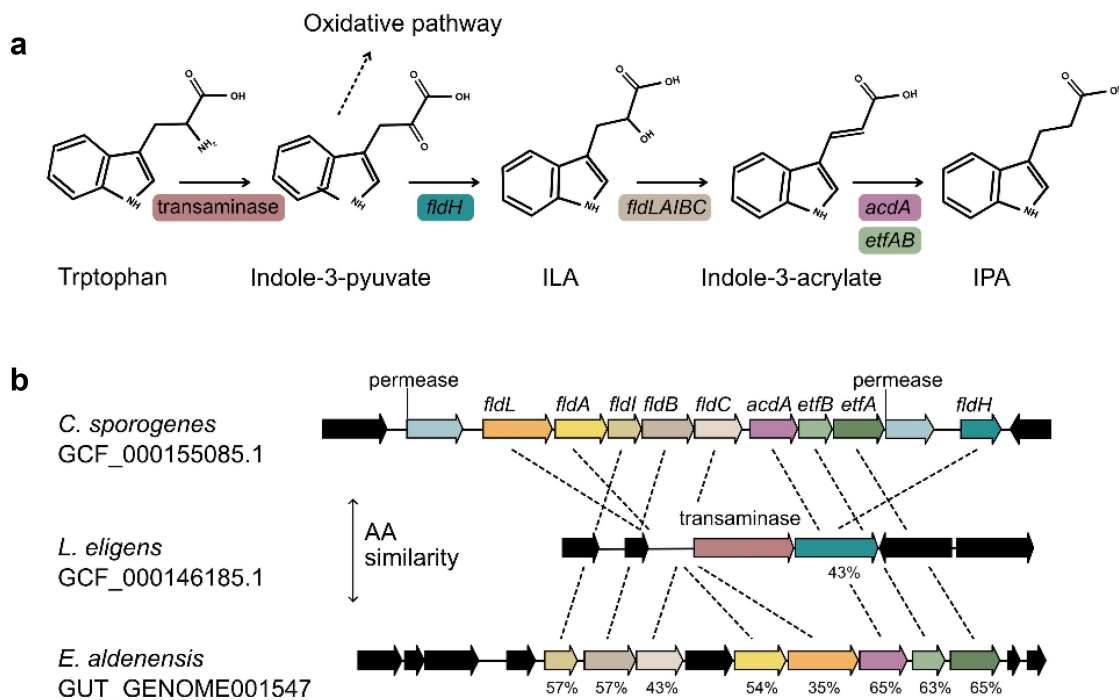
Figure 3. *C. sporogenes* genes in the reductive pathway of tryptophan metabolism and corresponding homologs in *E. aldenesis* and *L. eligens* genomes. (a) The reductive pathway starts with the conversion of indole-3-pyruvate to ILA by the phenyllactate dehydrogenase (*fldH*: CLOSPO_RS01525), followed by the conversion of ILA to indole-3-acrylate by the phenyllactate dehydratase enzyme complex (*fldLAIBC*: CLOSPO_RS01525-CLOSPO_RS01545), and finally the conversion of indole-3-acrylate to IPA by the acyl-CoA dehydrogenase (*acdA*: CLOSPO_RS01550). (b) The reductive pathway genes (CLOSPO_RS01525 to CLOSPO_RS01570) are arranged in a gene cluster in *C. sporogenes* ATCC 15579 (NCBI: GCF_000155085.1). The homolog with high amino acid sequence similarity (AA similarity %) for *fldH* in *L. eligens* DSM 3376 (NCBI: GCF_000146185.1) co-localizes with a transaminase (highlighted in red). Genes for homologous enzymes in *E. aldenesis* (HumGut: GUT_GENOME001547) form a similar cluster.

CLOSPO_RS01560 and CLOSPO_RS01555; Figure 3(b), Table S8).

By blasting the corresponding amino acid sequence against the Prokka-annotated genome of *L. eligens* DSM 3376 (genome GCF_000146185.1), we found a homolog for *fldH* with 43% amino acid sequence similarity (MCMENCIE_00178), which likely performs the dehydrogenation step from indole-3-pyruvate to ILA (Figure 3(b), Table S8). The *L. eligens fldH* co-localizes with a transaminase enzyme that may be responsible for the transamination of tryptophan to indole-3-pyruvate (MCMENCIE_00177; Figure 3(b), Table S8).

Since no genomes were available for the cultivated *E. aldenensis* strains, we used a high-quality *E. aldenensis* genome from the HumGut project (GUT_GENOME001547; Figure 3(b)).[52] A gene cluster for the transformation of ILA to IPA similar to the cluster in *C. sporogenes* was found, with homologs of high amino acid sequence similarity for the dehydratase activator (*fldI*; 57%; NJHLBJMC_04141), the acyl-CoA transferase (*fldA*; 54%; NJHLBJMC_04145) and the phenyllactate dehydratase subunits *fldB* (57%; NJHLBJMC_04142) and *fldC* (43%; NJHLBJMC_04143; Figure 3(b), Table S8). The co-localized homolog for the acyl-CoA ligase (*fldL*) was characterized by lower similarity (35%; NJHLBJMC_04146; Figure 3(b), Table S8). In addition, high sequence similarity (65%) was found for acyl-CoA dehydrogenase (*acdA*; NJHLBJMC_04147) and the electron transfer factors *etfA* (65%; NJHLBJMC_04149) and *etfB* (63%; NJHLBJMC_04148; Figure 3(b), Table S8).

We could not identify a homologous enzyme with high similarity and co-localization for *fldH* (maximum amino acid sequence similarity 35%, NJHLBJMC_00472; Table S8), which might explain the absence of IPA production from tryptophan in *E. aldenensis*.

Discussion

Although IPA is an important molecule in microbiota-host crosstalk, the microbial contributors and regulatory mechanisms shaping its production remain unclear. Using a cultivation-based approach, we combined metabolic and taxonomic screening of fecal microbiota from healthy adults with pure strain cultures. Fiber supplementation was used to selectively promote IPA levels and enrich associated taxa to facilitate their identification. Consequently, our data reflect the metabolic capacity and composition of the gut microbial community under these experimental conditions rather than its natural dynamics *in vivo*, which also involves host–microbiome interactions.

We first highlighted the modulatory effects of different dietary fibers on tryptophan metabolites in diverse, healthy gut microbiota. Fiber-mediated increases in reductive tryptophan metabolites and the reported decreases in indole (Figure 1, Figure S2-S3) align with findings from large human cohorts in which higher serum IPA was associated with fruit and legume consumption,[27,30,60] and decreased indoxyl sulfate levels (indole-derived uremic toxin) with fiber-rich food consumption.[61,62] In animal models, supplementation with specific fibers, including starch,[35,36] inulin,[63] pea[37] and pectin,[7,32,33] has been shown to promote IPA production. Consistently, our *ex vivo* data with human gut microbiota demonstrated that most tested fibers (*i.e.*, pectin, pea fiber, β-glucan, starch, dextrin, and arabinogalactan), could promote IPA production. Notably, pectin strongly enhanced IPA production in some donors but not others, suggesting that the baseline microbiota composition, and the presence or absence of specific taxa, may play a key role in this effect. In line, we showed that pectin increased the relative abundance of specific pectin-degrading taxa, including the newly identified ILA producer *L. eligens* (Figure S6).

Interestingly, we demonstrated that ILA is converted to IPA by all tested fecal cultures (*n* = 6; Figure 2(a)), supporting the idea that multi-species interactions involving ILA cross-feeding is a common mechanism contributing to the reductive tryptophan metabolism pathway. Under our experimental conditions, our data suggest that ILA production may be the limiting step in IPA biosynthesis and that promoting ILA levels and ILA-producing taxa (*e.g.*, via fiber supplementation) could enhance IPA production. Consistently, previous studies have reported fiber-mediated IPA increases without identifying known IPA producers. Instead, IPA levels correlated with taxonomic groups with ILA-producing potential, such as *Enterococcus* and *Lactococcus* in pigs or *Lactobacillus* in cats.[32,36] Similarly, IPA levels correlated with milk consumption and the abundance of potential ILA-producing *Bifidobacterium* in lactase-non-persistent individuals,[27,64] further highlighting ILA cross-feeding as a previously overlooked contributor to microbial IPA production. Finally, the importance of ILA cross-feeding in modulating inflammatory responses was recently reported in a colitis mouse model, where the supplementation of an ILA-producing *Lactobacillus* could rescue IPA production and alleviated inflammation.[26]

In addition to identifying the novel ILA producer *L. eligens*, we expand the list of known IPA producers (Tables S4–S5) by identifying *E. aldenensis*. Unlike previously known IPA producers, *E. aldenensis* can only produce IPA from ILA, but not tryptophan (Figure 2(b)). Consistently, *E. aldenensis* belongs to *Lachnospiraceae* and is phylogenetically distinct from other IPA-producing taxa (Figure S10B). The discovery of both *L. eligens* and *E. aldenensis* broadens the diversity of gut microbes involved in tryptophan metabolism, and highlighting their cross-feeding capability may help identify additional species with similar functions. Indeed, while the contribution of these species to *in vivo* IPA levels remains uncertain despite their high prevalence in the human population (>75%; Figure S10A), a homology-based search using the reductive pathway gene cluster from these new strains, coupled with targeted functional assays, could uncover additional ILA and IPA producers. Classifying IPA producers by their ability to utilize tryptophan or ILA may help elucidate the mechanisms underlying disease-associated declines in IPA levels. For instance, *Lachnospira* spp. are frequently depleted in Crohn's disease,[65] potentially reducing precursor availability for IPA production.

In addition to identifying novel IPA-producing species, it will be necessary to decipher how the metabolic activity of IPA producers is modulated

by environmental factors. The formation of tryptophan catabolites by individual strains is dependent on physicochemical parameters such as pH and the availability of *N*- and *C*-sources.[39,59] Competition for substrate may also play an important role in multi-species communities under conditions of low tryptophan availability. A recent study demonstrated that competition for tryptophan between IPA-producing *C. sporogenes* and indole-producing *Escherichia coli* was modulated by C-source availability.[7] The presence of pectin-derived monosaccharides suppressed indole formation by *E. coli* and resulted in higher tryptophan availability for IPA production by *C. sporogenes*, demonstrating an alternative mechanism by which fiber-rich diets, together with fiber-degrading species that release simple sugars, modulate the fate of tryptophan.[7]

Our findings are based on *in vitro* experiments, and further research is needed to determine the physiological relevance of *L. eligens* and *E. aldenensis* as ILA and IPA producers, as well as the observed cross-feeding interactions *in vivo*. Studies in animal models and human cohorts will be essential to assess their contribution to IPA production and its potential impact on host health. While these limitations should be considered, our study provides a foundation for future research into the tryptophan metabolic niche and offers a direction for targeted dietary interventions, probiotic strategies, or symbiotic approaches to enhance the production of health-promoting metabolites in the gut.

Disclosure statement

No potential conflict of interest was reported by the author(s).

ORCID

Benoit Pugin 🆔 http://orcid.org/0000-0001-7132-9477

Author contributions

BP, JZ, and CL conceptualized the project. JZ, BP and DM conceptualized and planned the experiment. JZ, MC, SP and DM performed the experiment and analysis. MK, BP, SP and JZ implemented the UHPLC method. SR provided support for genome analysis and performed the functional prediction analysis. JZ, BP, and CL interpreted the data. JZ and BP wrote the original draft of the manuscript. CL and BP provided financial support.

Data availability statement

Sequencing data from fecal microbiota cultures supplemented with tryptophan or ILA can be accessed from the EGA repository (accession number: EGAD50000000780) or from the NCBI repository (accession number PRJNA1136232), respectively.

References

1. Lavelle A, Sokol H. Gut microbiota-derived metabolites as key actors in inflammatory bowel disease. Nat Rev Gastroenterol Hepatol. 2020;17(4):223–237. doi: 10.1038/s41575-019-0258-z.
2. Liu J, Tan Y, Cheng H, Zhang D, Feng W, Peng C. Functions of gut microbiota metabolites, current status and future perspectives. Aging Dis. 2022;13(4):1106. doi: 10.14336/AD.2022.0104.
3. Wikoff WR, Anfora AT, Liu J, Schultz PG, Lesley SA, Peters EC, Siuzdak G. Metabolomics analysis reveals large effects of gut microflora on mammalian blood metabolites. Proc Natl Acad Sci USA. 2009;106 (10):3698. doi: 10.1073/pnas.0812874106.
4. Dodd D, Spitzer MH, Van Treuren W, Merrill BD, Hryckowian AJ, Higginbottom SK, Le A, Cowan TM, Nolan GP, Fischbach MA, et al. A gut bacterial pathway metabolizes aromatic amino acids into nine circulating metabolites. Nature. 2017;551(7682):648–652. doi: 10.1038/nature24661.
5. Dong F, Hao F, Murray IA, Smith PB, Koo I, Tindall AM, Kris-Etherton PM, Gowda K, Amin SG,

Patterson AD, et al. Intestinal microbiota-derived tryptophan metabolites are predictive of Ah receptor activity. Gut Microbes. 2020;12(1):1–24. doi: 10.1080/19490976.2020.1788899.

6. Lee JH, Lee J. Indole as an intercellular signal in microbial communities. FEMS Microbiol Rev. 2010;34 (4):426–444. doi: 10.1111/j.1574-6976.2009.00204.x.

7. Sinha AK, Basler M, Broz P, Dittrich PS, Drescher K, Egli A, Harms A, Hierlemann A, Hiller S, King CG, et al. Revitalizing antibiotic discovery and development through in vitro modelling of in-patient conditions. Nat Microbiol. 2024;9(1):1–3. doi: 10.1038/s41564-023-01566-w.

8. Williams BB, Van Benschoten A, Cimermancic P, Donia M, Zimmermann M, Taketani M, Ishihara A, Kashyap P, Fraser J, Fischbach M, et al. Discovery and characterization of gut microbiota decarboxylases that can produce the Neurotransmitter Tryptamine. Cell Host & Microbe. 2014;16(4):495–503. doi: 10.1016/j.chom.2014.09.001.

9. Otaru N, Greppi A, Plüss S, Zünd J, Mujezinovic D, Baur J, Koleva E, Lacroix C, Pugin B. Intestinal bacteria-derived tryptamine and its impact on human gut microbiota. Front Microbiomes. 2024;3:1373335. doi: 10.3389/frmbi.2024.1373335.

10. Roager HM, Licht TR. Microbial tryptophan catabolites in health and disease. Nat Commun. 2018;9(1):3294. doi: 10.1038/s41467-018-05470-4.

11. Banoglu E, Jha GG, King RS. Hepatic microsomal metabolism of indole to indoxyl, a precursor of indoxyl sulfate. Eur J Drug Metabol Pharmacokinet. 2001;26 (4):235–240. doi: 10.1007/BF03226377.

12. Wlodarska M, Luo C, Kolde R, d'Hennezel E, Annand JW, Heim CE, Krastel P, Schmitt EK, Omar AS, Creasey EA, et al. Indoleacrylic acid produced by commensal Peptostreptococcus species suppresses inflammation. Cell Host & Microbe. 2017;22 (1):25–37.e6. doi: 10.1016/j.chom.2017.06.007.

13. Bansal T, Alaniz RC, Wood TK, Jayaraman A. The bacterial signal indole increases epithelial-cell tight-junction resistance and attenuates indicators of inflammation. Proc Natl Acad Sci USA. 2010;107 (1):228–233. doi: 10.1073/pnas.0906112107.

14. Bhattarai Y, Jie S, Linden DR, Ghatak S, Mars RAT, Williams BB, Pu M, Sonnenburg JL, Fischbach MA, Farrugia G, et al. Bacterially derived tryptamine increases mucus release by activating a host receptor in a mouse model of inflammatory bowel disease. iScience. 2020;23(12):101798. doi: 10.1016/j.isci.2020.101798.

15. Alexeev EE, Dowdell AS, Henen MA, Lanis JM, Lee JS, Cartwright IM, Schaefer REM, Ornelas A, Onyiah JC, Vögeli B, et al. Microbial-derived indoles inhibit neutrophil myeloperoxidase to diminish bystander tissue damage. Faseb J. 2021;35(5):e21552. doi: 10.1096/fj.202100027R.

16. Venkatesh M, Mukherjee S, Wang H, Li H, Sun K, Benechet A, Qiu Z, Maher L, Redinbo M, Phillips R, et al. Symbiotic bacterial metabolites regulate gastrointestinal barrier function via the xenobiotic sensor PXR and Toll-like receptor 4. Immunity. 2014;41 (2):296–310. doi: 10.1016/j.immuni.2014.06.014.

17. Laursen MF, Sakanaka M, von Burg N, Mörbe U, Andersen D, Moll JM, Pekmez CT, Rivollier A, Michaelsen KF, Mølgaard C, et al. Bifidobacterium species associated with breastfeeding produce aromatic lactic acids in the infant gut. Nat Microbiol. 2021;6 (11):1367. doi: 10.1038/s41564-021-00970-4.

18. Zelante T, Iannitti R, Cunha C, De Luca A, Giovannini G, Pieraccini G, Zecchi R, D'Angelo C, Massi-Benedetti C, Fallarino F, et al. Article tryptophan catabolites from microbiota engage aryl hydrocarbon receptor and balance mucosal reactivity via interleukin-22. Immunity. 2013;39(2):372–385. doi: 10.1016/j.immuni.2013.08.003.

19. Nikolaus S, Schulte B, Al-Massad N, Thieme F, Schulte DM, Bethge J, Rehman A, Tran F, Aden K, Häsler R, et al. Increased tryptophan metabolism is associated with activity of inflammatory bowel diseases. Gastroenterology. 2017;153(6):1504–1516.e2. doi: 10.1053/j.gastro.2017.08.028.

20. Lamas B, Richard ML, Leducq V, Pham H-P, Michel M-L, Da Costa G, Bridonneau C, Jegou S, Hoffmann TW, Natividad JM, et al. CARD9 impacts colitis by altering gut microbiota metabolism of tryptophan into aryl hydrocarbon receptor ligands. Nat Med. 2016;22(6):598. doi: 10.1038/nm.4102.

21. Jackson MA, Verdi S, Maxan M-E, Shin CM, Zierer J, Bowyer RCE, Martin T, Williams FMK, Menni C, Bell JT, et al. Gut microbiota associations with common diseases and prescription medications in a population-based cohort. Nat Commun. 2018;9 (1):2655. doi: 10.1038/s41467-018-05184-7.

22. Sun XZ, Zhao D-Y, Zhou Y-C, Wang Q-Q, Qin G, Yao S-K. Alteration of fecal tryptophan metabolism correlates with shifted microbiota and may be involved in pathogenesis of colorectal cancer. World J Gastroenterol. 2020;26(45):7173. doi: 10.3748/wjg.v26.i45.7173.

23. Levi I, Gurevich M, Perlman G, Magalashvili D, Menascu S, Bar N, Godneva A, Zahavi L, Chermon D, Kosower N, et al. Potential role of indolelactate and butyrate in multiple sclerosis revealed by integrated microbiome-metabolome analysis. Cell Reports Med. 2021;2(4):100246. doi: 10.1016/j.xcrm.2021.100246.

24. Alexeev EE, Lanis JM, Kao DJ, Campbell EL, Kelly CJ, Battista KD, Gerich ME, Jenkins BR, Walk ST, Kominsky DJ, et al. Microbiota-derived indole metabolites promote human and murine intestinal homeostasis through regulation of interleukin-10 receptor. Am J Pathol. 2018;188(5):1183–1194. doi: 10.1016/j.ajpath.2018.01.011.

25. Lloyd-Price J, Arze C, Ananthakrishnan AN, Schirmer M, Avila-Pacheco J, Poon TW, Andrews E, Ajami NJ, Bonham KS, Brislawn CJ, et al. Multi-omics of the gut microbial ecosystem in inflammatory bowel diseases. Nature. 2019;569(7758):655–662. doi: 10.1038/s41586-019-1237-9.

26. Wang G, Fan Y, Zhang G, Cai S, Ma Y, Yang L, Wang Y, Yu H, Qiao S, Zeng X, et al. Microbiota-derived indoles alleviate intestinal inflammation and modulate microbiome by microbial cross-feeding. Microbiome. 2024;12(1):59. doi: 10.1186/s40168-024-01750-y.

27. Qi Q, Li J, Yu B, Moon J-Y, Chai JC, Merino J, Hu J, Ruiz-Canela M, Rebholz C, Wang Z, et al. Host and gut microbial tryptophan metabolism and type 2 diabetes: an integrative analysis of host genetics, diet, gut microbiome and circulating metabolites in cohort studies. Gut. 2022;71(6):1095. doi: 10.1136/gutjnl-2021-324053.

28. De Mello VD, Paananen J, Lindström J, Lankinen MA, Shi L, Kuusisto J, Pihlajamäki J, Auriola S, Lehtonen M, Rolandsson O, et al. Indole propionic acid and novel lipid metabolites are associated with a lower risk of type 2 diabetes in the Finnish diabetes prevention study. Sci Rep. 2017;7(1):46337. doi: 10.1038/srep46337.

29. Menni C, Hernandez MM, Vital M, Mohney RP, Spector TD, Valdes AM. Circulating levels of the anti-oxidant indoleproprionic acid are associated with higher gut microbiome diversity. Gut Microbes. 2019;10(6):688–695. doi: 10.1080/19490976.2019.1586038.

30. Tuomainen M, Lindström J, Lehtonen M, Auriola S, Pihlajamäki J, Peltonen M, Tuomilehto J, Uusitupa M, de Mello VD, Hanhineva K, et al. Associations of serum indole propionic acid, a gut microbiota metabolite, with type 2 diabetes and low-grade inflammation in high-risk individuals. Nutr Diabetes. 2018;8(1):35. doi: 10.1038/s41387-018-0046-9.

31. Knarreborg A, Beck J, Jensen MT, Laue A, Agergaard N, Jensen BB. Effect of non-starch polysaccharides on production and absorption of indolic compounds in entire male pigs. Anim Sci. 2002;74(3):445–453. doi: 10.1017/S1357729800052590.

32. Dang G, Wen X, Zhong R, Wu W, Tang S, Li C, Yi B, Chen L, Zhang H, Schroyen M, et al. Pectin modulates intestinal immunity in a pig model via regulating the gut microbiota-derived tryptophan metabolite-AhR-IL22 pathway. J Anim Sci Biotechnol. 2023;14(1):38. doi: 10.1186/s40104-023-00838-z.

33. Wang Q, Li Y, Lv L, Jiang H, Yan R, Wang S, Lu Y, Wu Z, Shen J, Jiang S, et al. Identification of a protective Bacteroides strain of alcoholic liver disease and its synergistic effect with pectin. Appl Microbiol Biotechnol. 2022;106(9–10):3735–3749. doi: 10.1007/s00253-022-11946-7.

34. Huang Z, Boekhorst J, Fogliano V, Capuano E, Wells JM. Distinct effects of fiber and colon segment on microbiota-derived indoles and short-chain fatty acids. Food Chem. 2023;398:133801. doi: 10.1016/j.foodchem.2022.133801.

35. Koay YC, Wali JA, Luk AWS, Macia L, Cogger VC, Pulpitel TJ, Wahl D, Solon-Biet SM, Holmes A, Simpson SJ, et al. Ingestion of resistant starch by mice markedly increases microbiome-derived metabolites. Faseb J. 2019;33(7):8033–8042. doi: 10.1096/fj.201900177R.

36. Jackson MI, Waldy C, Jewell DE, Loor JJ. Dietary resistant starch preserved through mild extrusion of grain alters fecal microbiome metabolism of dietary macronutrients while increasing immunoglobulin a in the cat. PLOS ONE. 2020;15(11):e0241037. doi: 10.1371/journal.pone.0241037.

37. Yu M, Li Z, Rong T, Tian Z, Deng D, Lu H, Zhang R, Ma X. Integrated metagenomics-metabolomics analysis reveals the cecal microbial composition, function, and metabolites of pigs fed diets with different starch sources. Food Res Int. 2022;154:110951. doi: 10.1016/j.foodres.2022.110951.

38. Pan T, Pei Z, Fang Z, Wang H, Zhu J, Zhang H, Zhao J, Chen W, Lu W. Uncovering the specificity and predictability of tryptophan metabolism in lactic acid bacteria with genomics and metabolomics. Front Cell Infect Microbiol. 2023;13:1154346. doi: 10.3389/fcimb.2023.1154346.

39. Russell WR, Duncan SH, Scobbie L, Duncan G, Cantlay L, Calder AG, Anderson SE, Flint HJ. Major phenylpropanoid-derived metabolites in the human gut can arise from microbial fermentation of protein. Mol Nutr Food Res. 2013;57(3):523–535. doi: 10.1002/mnfr.201200594.

40. Elsden SR, Hilton MG, Waller JM. The end products of the metabolism of aromatic amino acids by clostridia. Arch Microbiol. 1976;107(3):283–288. doi: 10.1007/BF00425340.

41. Smith EA, Macfarlane GT. Enumeration of human colonic bacteria producing phenolic and indolic compounds: effects of pH, carbohydrate availability and retention time on dissimilatory aromatic amino acid metabolism. J Appl Bacteriol. 1996;81(3):288–302. doi: 10.1111/j.1365-2672.1996.tb04331.x.

42. Zünd JN, Plüss S, Mujezinovic D, Menzi C, von Bieberstein PR, de Wouters T, Lacroix C, Leventhal GE, Pugin B. A flexible high-throughput cultivation protocol to assess the response of individuals' gut microbiota to diet-, drug-, and host-related factors. ISME Commun. 2024;4(1):ycae035. doi: 10.1093/ismeco/ycae035.

43. Konopelski P, Konop M, Gawrys-Kopczynska M, Podsadni P, Szczepanska A, Ufnal M. Indole-3-propionic acid, a tryptophan-derived bacterial metabolite, reduces weight gain in rats. Nutrients. 2019;11(3):591. doi: 10.3390/nu11030591.

44. Otaru N, Ye K, Mujezinovic D, Berchtold L, Constancias F, Cornejo FA, Krzystek A, de Wouters T, Braegger C, Lacroix C, et al. GABA

production by human intestinal bacteroides spp.: prevalence, regulation, and role in acid stress tolerance. Front Microbiol. 2021;12:656895. doi: 10.3389/fmicb. 2021.656895.

45. Constancias F, Mahé F. fconstancias/metabaRpipe: v0.9 (v0.9). Zenodo; 2022. doi: 10.5281/zenodo.6423397.

46. Callahan BJ, McMurdie PJ, Rosen MJ, Han AW, Johnson AJA, Holmes SP. DADA2: high-resolution sample inference from illumina amplicon data. Nat Methods. 2016;13(7):581–583. doi: 10.1038/nmeth. 3869.

47. Quast C, Pruesse E, Yilmaz P, Gerken J, Schweer T, Yarza P, Peplies J, Glöckner FO. The SILVA ribosomal RNA gene database project: improved data processing and web-based tools. Nucleic Acids Res. 2013;41(D1): D590–D596. doi: 10.1093/nar/gks1219.

48. Yilmaz P, Parfrey LW, Yarza P, Gerken J, Pruesse E, Quast C, Schweer T, Peplies J, Ludwig W, Glöckner FO, et al. The SILVA and "all-species living tree project (LTP)" taxonomic frameworks. Nucleic Acids Res. 2014;42(D1):D643–D648. doi: 10.1093/nar/gkt1209.

49. McMurdie PJ, Holmes S, Watson M. Phyloseq: an R package for reproducible interactive analysis and graphics of microbiome census data. PLOS ONE. 2013;8(4):e61217. doi: 10.1371/journal.pone.0061217.

50. Barnett DJM, Arts ICW, Penders J. microViz: an R package for microbiome data visualization and statistics. J Open Source Softw. 2021;6(63):3201. doi: 10.21105/joss.03201.

51. Camacho C, Coulouris G, Avagyan V, Ma N, Papadopoulos J, Bealer K, Madden TL. BLAST+: architecture and applications. BMC Bioinf. 2009;10(1):421. doi: 10.1186/1471-2105-10-421.

52. Hiseni P, Rudi K, Wilson RC, Hegge FT, Snipen L. HumGut: a comprehensive human gut prokaryotic genomes collection filtered by metagenome data. Microbiome. 2021;9(1):165. doi: 10.1186/s40168-021-01114-w.

53. Seemann T. Prokka: rapid prokaryotic genome annotation. Bioinformatics. 2014;30(14):2068–2069. doi: 10.1093/bioinformatics/btu153.

54. Ernst FGM, Shetty SA, Borman T, Lahti L. Mia: microbiome analysis. R Package Version 1.11.5. 2024. https:// github.com/microbiome/mia .

55. Chung WSF, Meijerink M, Zeuner B, Holck J, Louis P, Meyer AS, Wells JM, Flint HJ, Duncan SH. Prebiotic potential of pectin and pectic oligosaccharides to promote anti-inflammatory commensal bacteria in the human colon. FEMS Microbiol Ecol. 2017;93(11):127. doi: 10.1093/femsec/fix127.

56. Flint HJ, Scott KP, Duncan SH, Louis P, Forano E. Microbial degradation of complex carbohydrates in the gut. Gut Microbes. 2012;3(4):289. doi: 10.4161/ gmic.19897.

57. Noel M, Mayeur-Nickel F, Wiart-Letort S, Grundy MML. Pea cell wall polysaccharides and their structural integrity influence protein bioaccessibility and hydrolysis. J Funct Foods. 2024;112:105986. doi: 10.1016/j.jff.2023.105986.

58. Dickert S, Pierik AJ, Buckel W. Molecular characterization of phenyllactate dehydratase and its initiator from Clostridium sporogenes. Mol Microbiol. 2002;44 (1):49–60. doi: 10.1046/j.1365-2958.2002.02867.x.

59. Liu Y, Chen H, Van Treuren W, Hou B-H, Higginbottom SK, Dodd D. Clostridium sporogenes uses reductive Stickland metabolism in the gut to generate ATP and produce circulating metabolites. Nat Microbiol. 2022;7(5):695–706. doi: 10.1038/s41564-022-01109-9.

60. Pallister T, Jennings A, Mohney RP, Yarand D, Mangino M, Cassidy A, MacGregor A, Spector TD, Menni C, et al. Characterizing blood metabolomics profiles associated with self-reported food intakes in female twins. PLOS ONE. 2016;11(6):e0158568. doi: 10.1371/journal.pone.0158568.

61. Sirich TL, Plummer NS, Gardner CD, Hostetter TH, Meyer TW. Effect of increasing dietary fiber on plasma levels of colon-derived solutes in hemodialysis patients. Clin J Am Soc Nephrol. 2014;9(9):1603. doi: 10.2215/ CJN.00490114.

62. Yang HL, Feng P, Xu Y, Hou Y-Y, Ojo O, Wang X-H. The role of dietary fiber supplementation in regulating uremic toxins in patients with chronic kidney disease: a meta-analysis of randomized controlled trials. J Ren Nutr. 2021;31(5):438–447. doi: 10.1053/j.jrn.2020.11. 008.

63. Arifuzzaman M, Won TH, Li T-T, Yano H, Digumarthi S, Heras AF, Zhang W, Parkhurst CN, Kashyap S, Jin W-B, et al. Inulin fibre promotes microbiota-derived bile acids and type 2 inflammation. Nature. 2022;611(7936):578–584. doi: 10.1038/s41586-022-05380-y.

64. Luo K, Chen G-C, Zhang Y, Moon J-Y, Xing J, Peters BA, Usyk M, Wang Z, Hu G, Li J, et al. Variant of the lactase LCT gene explains association between milk intake and incident type 2 diabetes. Nat Metab. 2024;6(1):169. doi: 10.1038/s42255-023-00961-1.

65. Abdel-Rahman LIH, Morgan XC. Searching for a consensus among inflammatory bowel disease studies: a systematic meta-analysis. Inflamm Bowel Dis. 2023;29 (1):125–139. doi: 10.1093/ibd/izac194.